



Science Arts & Métiers (SAM)

is an open access repository that collects the work of Arts et Métiers Institute of Technology researchers and makes it freely available over the web where possible.

This is an author-deposited version published in: <https://sam.ensam.eu>
Handle ID: <http://hdl.handle.net/10985/19979>

To cite this version :

Mohammadali SHIRINBAYAN - Multiscale damage analysis of the tension-tension fatigue behavior of a low-density sheet molding compound - Journal of Applied Polymer Science - Vol. 138, n°4, p.1-12 - 2021

Any correspondence concerning this service should be sent to the repository

Administrator : archiveouverte@ensam.eu



Multiscale damage analysis of the tension-tension fatigue behavior of a low-density sheet molding compound

Mohammadali Shirinbayan^{1,2} 

¹Arts et Metiers Institute of Technology, CNRS, CNAM, PIMM, HESAM University, Paris, France

²Arts et Metiers Institute of Technology, CNRS, CNAM, LIFSE, HESAM University, Paris, France

Correspondence

Mohammadali Shirinbayan, Arts et Metiers Institute of Technology, CNRS, CNAM, PIMM, HESAM University, F-75013 Paris, France.
Email: mohammadali.shirinbayan@ensam.eu

Abstract

This article presents the experimental findings of tension-tension stress-controlled fatigue tests performed on low-density sheet molding compound (LD-SMC). LD-SMC composite is a type of SMC including a polyester resin reinforced with chopped glass fibers bundles and hollow glass spheres. The coupled frequency-amplitude affects the nature of the overall fatigue response, which can be controlled by the damage mechanisms accumulation and/or by the self-heating. In fact, the self-heating produced a material softening and decreased the fatigue lifetime. For fatigue loading at 80 Hz, self-heating has been observed and yielded to a temperature rise to 65°C, which is more than a glass transition temperature of polyester. Thus, the polyester matrix is subjected to remarkable thermally activated modifications of its physical state. Multiscale damage analysis of the randomly-oriented sample in fatigue showed that the first observed damage phenomenon corresponds to the debonding of the hollow glass microspheres occurring in the fiber depleted zones.

KEYWORDS

composites, fibers, glass transition, SMC, thermosets

1 | INTRODUCTION

In recent years, the industry tendency has been toward the materials with low weight and high mechanical properties. On the other hand, high strength to weight ratio for materials used in the automotive industry is an essential factor.^{1–3}

Sheet molding compounds (SMCs) have wide application fields in aerospace, agricultural, rail and marine, and building and construction, but SMCs fabrication has been motivated mostly by the automotive industry.^{2,4} Moreover, among the advantages of SMCs, the ability to adjust their formulations is very interesting.^{5–7} The composite matrix of SMCs is a combination of polyester, vinylester or epoxy as a thermosetting resin, fillers such as alumina, calcium carbonate, and thickeners, referred to as additives.^{1–8} A variety of fiber reinforcement can be used including glass

or carbon fibers with a volume fraction between 10% and 65%.

Low-density sheet molding compounds (LD-SMCs) have been developed mainly based on hollow glass microspheres (HGMs). By density reduction of 20%–30% using HGMs in SMC composites, Young's modulus can be reduced.^{1,2,9} Oldenbo et al.⁹ investigated that the mechanical behavior of Flex SMC, a new type of SMC that contains HGMs with additives, in comparison with a conventional SMC (Std. SMC). It has been observed that Flex SMC has higher impact resistance and higher fracture toughness with the lower density. In the framework of the lightening of structures, these materials present an excellent alternative to replace certain light alloys given the design of automotive parts with complex geometries.

To formulate the equation of SMC composites, it is necessary to have enough information about mechanical

properties and especially damage phenomena under different modes of loading such as monotonic or fatigue.^{10,11}

Fatigue response of composites is usually characterized by the Wöhler curve, which is a curve giving the value of cyclic stress/strain amplitude versus the number of cycles to failure, N .^{2,12–16} The parameters that can affect the cyclic behavior are fiber orientations, applied stress/strain, temperature, frequency, and self-heating.^{2,14–16} Strain rate and temperature are two important parameters, which effect on material behavior under different solicitation modes such as tension, compression, shear, and torsion.¹⁷

The viscoelastic behavior of the matrix is another essential aspect. In the case of an SMC composite with the thermosetting matrix, one generally speaks about a visco-elasto-damageable behavior.^{18–21} On the other hand, in the case of thermoplastic matrices, there is a coupling between the viscoplasticity coming from the matrix and the damage.²²

In general, the damage is defined as a set of microstructural changes inside of the material that causes irreversible mechanical degradation. In SMCs, the best-known damage mechanisms are matrix cracking, interfacial debonding: the interface between fibers and matrix, pull out or tearing, fiber breakage and delamination between layers for laminated composites.^{10,17,22–24} The risk of these damages is that they are sometimes undetectable to the naked eye as their location internal to the structure. Depending on the distribution and the geometry of the components in the matrix, the SMC composite will exhibit anisotropic behavior.

Generally, three scales are necessary for the study of damage in SMC composites.^{25,26} The microscopic scale that determines the finest heterogeneities present in the material. The analysis of these local mechanisms of damage and deformation is generally done by in situ tests under a scanning electron microscope (SEM).^{27,28} The interest of this type of test is to be able to observe in real time the damage mechanisms, which intervene during loading, their threshold, and their kinetics of evolution. Recently developed, in situ tests can also be carried out in a microtomography^{27–29} and thus make it possible to follow the evolution of the damage not only on the surface of the test piece but also in volume.

The macroscopic scale considers the structure homogeneous. At the macroscopic scale, the damage often results in a progressive decrease in stiffness followed by the failure of the composite. The mesoscopic scale is intermediate between the two previous scales. This scale does not see the finest heterogeneities and it considers the fold of stratification as a homogeneous entity.^{25,26}

Distinguish the damage in composite by the Young modulus evaluation seems to be sufficiency to describe

the different mechanisms that contribute to failure in monotonic and fatigue loadings. One can define a macroscopic damage variable as $D = 1 - E_D/E_0$, where E_0 and E_D are Young's modulus of the virgin and damaged material, respectively.^{18–21} In the case of SMC materials, there are few experimental results on fatigue behavior. Tamboura et al.³⁰ studied the evolution of the densities of interfacial cracks during fatigue loading thanks to interrupted tests with follow-up of the damage on a microscopic scale by SEM. This study has further demonstrated that damage to the fiber-matrix interface is the primary driver of damage. The initiation and propagation of this mechanism have been quantitatively characterized along with several reinforcement directions.

Fleckenstein et al.³¹ studied the effect of preferred fiber orientations of SMC under fatigue loading. They showed that the specimens with predominantly 0° fiber alignment have the highest fatigue strength. Wang et al.³² concluded that increasing the applied fatigue stress, σ_{\max} , leads to a higher stiffness reduction rate and shorter fatigue lifetime.

Coupled effect of the cyclic loading amplitude and frequency on the fatigue behavior of advanced SMC (A-SMC) and the induced self-heating phenomenon have been studied by Shirinbayan et al.² They showed that for the high values of applied stress and frequency, the A-SMC exhibits an overall fatigue response mainly governed by the induced thermal fatigue (ITF) nature during the first stage corresponding to low cycles. The mechanical fatigue (MF) nature becomes predominant during the second stage before the failure. For low applied amplitude and frequency, no significant self-heating phenomenon has been observed.

In the present article, an experimental study is carried-out to widely investigate the influence of fiber orientation as well as the coupled effect of the cyclic loading amplitude and frequency on the fatigue behavior of a LD-SMC provided by the Plastic Omnium Auto Exterior. Special issues of this article concern multiscale damage analysis on the overall behaviors of this material under fatigue loading. This multiscale damage analysis has been performed to emphasize the effect of the presence of HGMs. Randomly-oriented (RO) fibers and highly-oriented (HO) fibers microstructures were prepared for physical, damage, and mechanical characterizations. For HO samples, two tensile directions were selected due to microstructure to evaluate the anisotropic effect: HO- 0° (parallel to the mold flow direction [MFD]) and HO- 90° (perpendicular to the MFD).

The main structure of this work is as follows: the section of material description and methods is dedicated to a description of the main physical characteristics and the modeling of the viscoelastic behavior of LD-SMC

composite using the dynamic mechanical analysis (DMA) test. The developed experimental procedure for fatigue testing at several frequencies has been performed. In experimental results and discussion section, experimental results obtained under quasistatic and fatigue loadings and multiscale damage analysis are presented and discussed.

2 | MATERIAL DESCRIPTION AND METHODS

2.1 | Low-density sheet molding compound

LD-SMC composite is a type of SMC reinforced with chopped glass fibers bundles with a length of 25 mm and hollow glass spheres (HGSs). In the compression molding process of LD-SMC, raw materials on rolls should be cut to a specific size and put into the mold under high temperature between 145 and 155°C and pressure between 80 and 120 bars. These process conditions lead to reducing the viscosity and allow fulfilling the whole cavity of the mold. After a short duration without any reticulation, the next step of the process consists of a reticulation time of the thermoset material that is the consolidation phase.

The LD-SMC composition is presented in Table 1. The Plastic Omnium Auto Exterior has provided RO and HO plates. HO plates have been achieved by an initial charge put only in the left part of a rectangular mold (30 × 40 cm²) before compression leading to material flow. RO plates were achieved without material flow by filling the mold.

2.2 | Methods of characterization and experimental procedure

2.2.1 | Microscopic observation

Microscopic observations and image analysis, using SEM (HITACHI 4800 SEM), have been done in order to

TABLE 1 LD-SMC composition

Product nature	Composition (in mass percent) (%)
Glass fibers	30
Hollow glass spheres	22
Polyester resin	12
Filler	32
Other products	4

Abbreviation: LD-SMC, low-density sheet molding compound.

qualitatively examine the composite microstructure and especially fibers orientation and damage analysis.

2.2.2 | DMA measurement

DMA tests have been attained to measure the main transitions temperatures on RO LD-SMC samples using the DMA Q800 instrument from TA Company. The DMA tests with 3-point bending mode have been realized at the following condition: temperature range varying from −100 to 250°C, temperature rate of 2°C/min, and a frequency of 1 Hz.

2.2.3 | Quasistatic tensile test

Quasistatic tensile experiments were achieved using the MTS 830 hydraulic machine with a loading cell of 10 kN under a loading velocity of 2 mm/min.

2.2.4 | Fatigue test

Tension-tension stress-controlled fatigue tests have been performed at different applied maximum stress (σ_{\max}) on MTS 830 hydraulic fatigue machine. The minimum applied stress (σ_{\min}) is always chosen to be equal to 10% of the maximum applied stress. The chosen stress-ratio is thus ($R_{\sigma} = 0.1$), and the range of applied stress level was chosen from 30 to 80 MPa.

In this article, the results of experiments performed at different frequencies, namely 10, 30, and 80 Hz are presented. During fatigue loading, the temperature rise, due to the composite self-heating, has been measured on the surface of the specimen using an infrared camera (Raynger-MX4). Tensile and fatigue tests were performed on the LD-SMC samples with the geometry presented in Figure 1.

2.2.5 | Multiscale damage analysis in fatigue

The macroscopic damage evolutions have been estimated through the measurement of Young's modulus evolutions. Microscopic damage observations were performed by subjecting the RO LD-SMC specimens into a fatigue loading under specific loading amplitude with a frequency of 10 Hz. To reduce the relaxation effect in the material, the observation time was limited to 15 minutes. The observation area corresponded to a polished thickness surface of the rectangular composite with a geometry is presented in Figure 2.

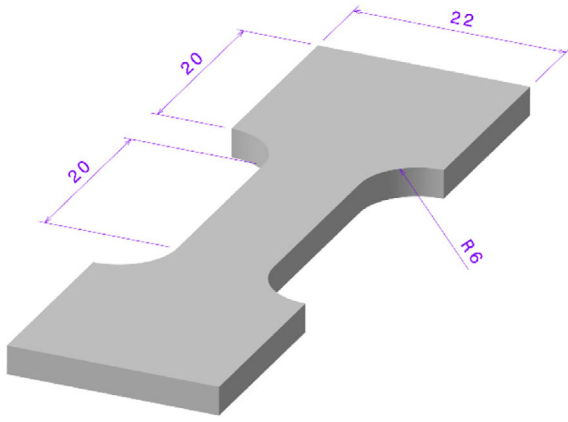


FIGURE 1 Specimen geometry and its related dimensions (in mm) for tensile and fatigue tests [Color figure can be viewed at wileyonlinelibrary.com]

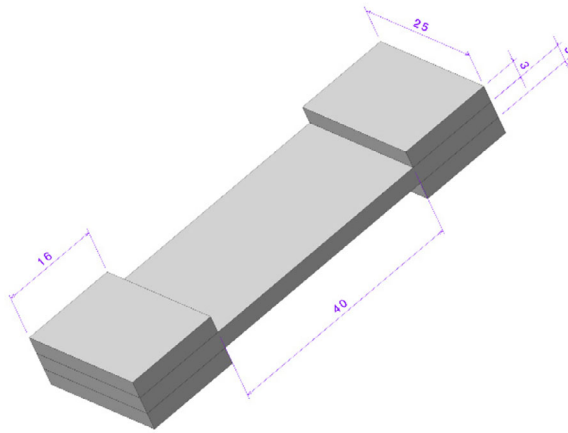


FIGURE 2 Specimen geometry (in mm) for damage analysis in fatigue [Color figure can be viewed at wileyonlinelibrary.com]

3 | EXPERIMENTAL RESULTS AND DISCUSSION

3.1 | Microstructure analysis

Before presenting the results of microstructure analysis, hydrostatic weighing method was used to measure the density. The results confirmed that the density of LD-SMC, $\sim 1.22 \text{ g/cm}^3$, is lower than the density of the standard SMC of 1.75 g/cm^3 . The analysis shows about 30% reduction of density because of adding HGSs. For RO LD-SMC, the homogeneous distribution of HGSs (Figure 3) is observed. To show the position of HGSs, the ImageJ software was used.

Figure 4 shows the microstructure of the LD-SMC plate after cutting in two directions of parallel or perpendicular to the MFD. The HO sample presents more fibers oriented in the MFD compared with the RO distribution of fibers (RO).

3.2 | Thermomechanical properties

3.2.1 | Glass transition temperature

Main transition temperatures due to molecular mobility as a function of the temperature have been measured using the DMA test. This test can be useful to analyze the induced self-heating phenomenon and to relate it to the measured temperature rise during a fatigue test at different amplitudes and frequencies. Figure 5 shows the evolution of the storage and loss moduli versus temperature on RO LD-SMC samples. As it can be noticed, LD-SMCs present the α -transition, related to the glass transition of nearly 50°C . The presence of HGSs and their breakage may cause the sudden drop of the elastic modulus in the glass transition region.

The elastic or viscous response of LD-SMC composite can be measured as a function of temperature using DMA; additionally, it is possible to understand the true internal damping of the system. One can suppose that LD-SMCs have rigidly stability at ambient temperature while the storage modulus continues to decrease slowly until 250°C due to the increase of macromolecular chain mobility.

3.2.2 | Viscoelasticity modeling by Cole-Cole principle

Various approaches have been utilized to study the viscoelastic properties in the temperature range between the glassy and rubbery domain, and different models have been proposed to predict these properties. These models generally represent the curve of E'' (loss modulus) as a function of E' (storage modulus), and the curve is known as the Cole-Cole diagram.^{33–35} For the validation of the theoretical model, experimental data obtained by the dynamic mechanical thermal analysis (DMA) tests are required. After DMA tests, an asymmetric Cole-Cole diagram has been plotted (Figure 6). According to the Perez model,³³ the behavior of polymers can be explained by the biparabolic model presented by the following equation:

$$E^* = E_0 + \frac{E_\infty - E_0}{1 + (i\omega\tau)^K + Q(i\omega\tau)^{K'}} = E' + iE'' \quad (1)$$

With

$$E' = E_0 + (E_\infty - E_0) \frac{1 + \cos\left(\frac{K\pi}{2}\right)(\omega\tau)^{-K} + Q\cos\left(\frac{K'\pi}{2}\right)(\omega\tau)^{-K'}}{D}, \quad (2)$$

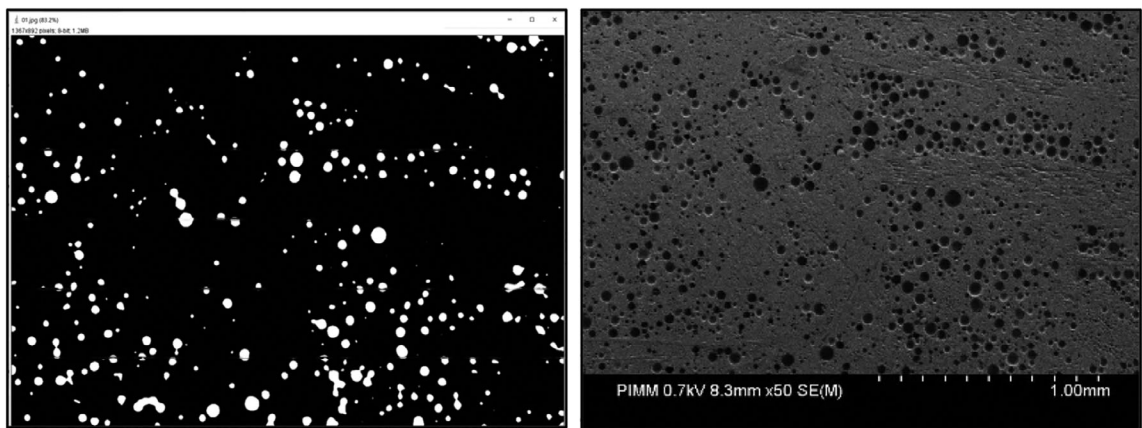
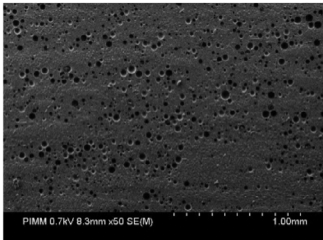
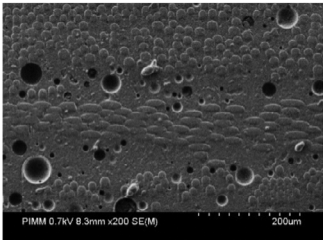
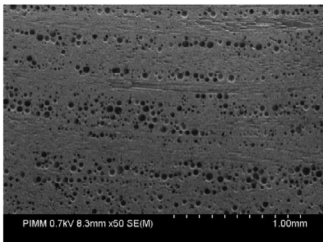
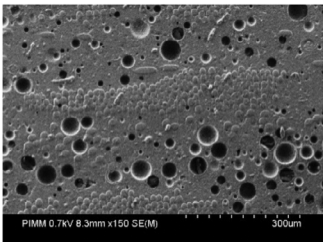


FIGURE 3 The microstructure of randomly-oriented low-density sheet molding compound: Homogeneous presence of hollow glass spheres

FIGURE 4 The microstructure of LD-SMC: Bundle of fibers and hollow glass spheres. HO, highly-oriented; LD-SMC, low-density sheet molding compound; MFD, mold flow direction; RO, randomly-oriented

LD-SMC	Parallel to MFD view	Perpendicular to MFD view
RO		
HO		

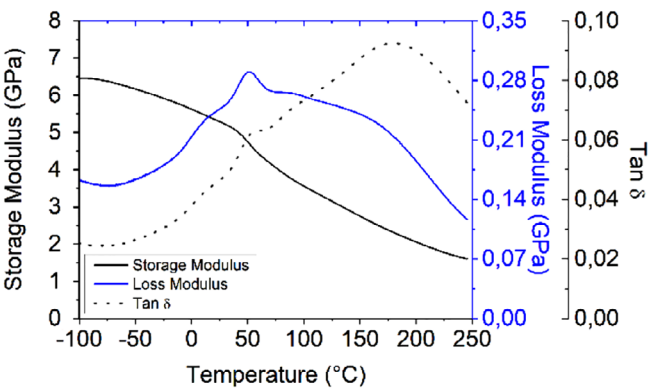


FIGURE 5 Dynamic mechanical analysis test result: Evolution of the storage and loss moduli versus temperature [Color figure can be viewed at wileyonlinelibrary.com]

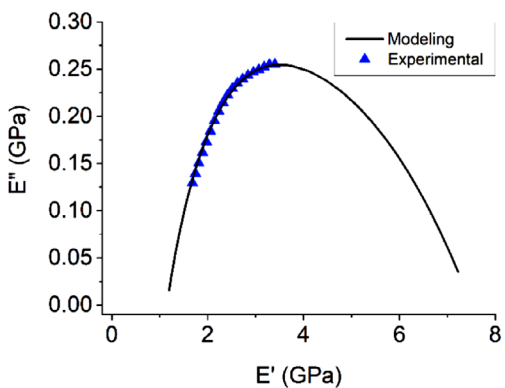


FIGURE 6 Cole-Cole plot of randomly-oriented low-density sheet molding compound composite [Color figure can be viewed at wileyonlinelibrary.com]

$$E'' = (E_\infty - E_0) \frac{\sin\left(\frac{k\pi}{2}\right)(\omega\tau)^{-K} + Q\sin\left(\frac{k'\pi}{2}\right)(\omega\tau)^{-K'}}{D}, \quad (3)$$

and

$$D = \left[1 + \cos\left(\frac{k\pi}{2}\right)(\omega\tau)^{-K} + Q\cos\left(\frac{k'\pi}{2}\right)(\omega\tau)^{-K'} \right]^2 + \left[\sin\left(\frac{k\pi}{2}\right)(\omega\tau)^{-K} + Q\sin\left(\frac{k'\pi}{2}\right)(\omega\tau)^{-K'} \right]^2, \quad (4)$$

where k and k' and Q are the constants of this model. $\omega = 2\pi f$ is the angular frequency (f = frequency). Furthermore, E^* is the complex shear modulus: E_∞ and E_0 are the value of modulus at the, respectively, glassy and rubbery states. k and k' depend on the slope of the tangents at the beginning and the end of the Cole-Cole diagram (dE''/dE'), Q is a constant related to the maximum value of E'' . τ is the average relaxation time.

The values of the model's parameters are shown in Table 2. The theoretical curve fits perfectly with the experimental results, signifying that the biparabolic model can accurately predict the viscoelastic behavior of RO LD-SMC.

3.3 | Quasistatic tensile behavior

3.3.1 | Effect of the fiber orientation distribution

Figure 7(a) illustrates the results of quasistatic tensile tests on HO-0°, RO, and HO-90° LD-SMC samples at room temperature. The value of Young's modulus of HO-0° is about 12 GPa, which is higher than those of RO (10 GPa) and HO-90° (9 GPa) samples. The failure of stress also highly depends on the fiber orientation. Failure stress of HO-0° is about four times higher than that of HO-90° samples, which confirms the dependency of failure stress on the fiber's orientation.

The threshold and kinetic of damage can be characterized by the evolution of the well-known scalar damage parameter ($D = 1 - E_D/E_0$). The residual Young's modulus after damage, E_D , is measured by a "loading-unloading" test in which reached the value of stress

increases at each reloading stage. Figure 7(b) shows the evolution of the macroscopic damage parameter against the stress level for the three kinds of specimen: HO-0°, RO, HO-90°.

HO-0° has the lowest damage parameter evolution. For example, in the case of HO-0° samples, macroscopic damage starts at a stress level of about 40 MPa, significantly higher than those of RO and HO-90° samples (corresponding to 28 and 18 MPa, respectively). Moreover, by increasing fiber orientation in the load direction damage threshold value is increased, and kinetic of damage propagation is decreased.

Evidently, in the macroscopic scale, HO-0° presents the good ability against the damage during the tensile test. Tensile properties of LD-SMCs are given in Table 3.

3.4 | Fatigue behavior analysis

3.4.1 | Effect of the fiber orientation distribution

Figure 8 shows the Wöhler curves obtained in tension-tension stress-controlled fatigue tests at a frequency of 30 Hz for HO-0°, RO, and HO-90° LD-SMC samples.

The curves evidence the effect of the fiber orientation distribution. In the case of RO samples for applied stress equal to 40 MPa, the fatigue life is about 300,000 cycles whereas the fatigue life is about 1000 cycles for applied stress of 60 MPa. Therefore, a variation of 33% in applied stress leads to fatigue life about 300 times higher. Figure 8 also demonstrates that the fatigue life for HO-90° samples is significantly affected, compared to those of the RO and HO-0° samples. Consequently, it can be proved that the fatigue life is strongly influenced by the fiber orientation. It can be established thus that for LD-SMC composite, the fatigue design can be efficiently optimized through fiber orientation with a critical reduction of material properties in the transverse direction.

3.4.2 | Effect of frequency

Wöhler curves obtained from fatigue tests for the frequencies of 10, 30, and 80 Hz in the case of HO-0° samples are shown in Figure 9. There is a small difference

Frequencies (Hz)	E_0 (MPa)	E_∞ (MPa)	k	k'	Q	τ (s)
1	1150	7500	0.23	0.084	2.2	0.95

TABLE 2 Perez model parameters for RO LD-SMC

Abbreviations: LD-SMC, low-density sheet molding compound; RO, randomly-oriented.

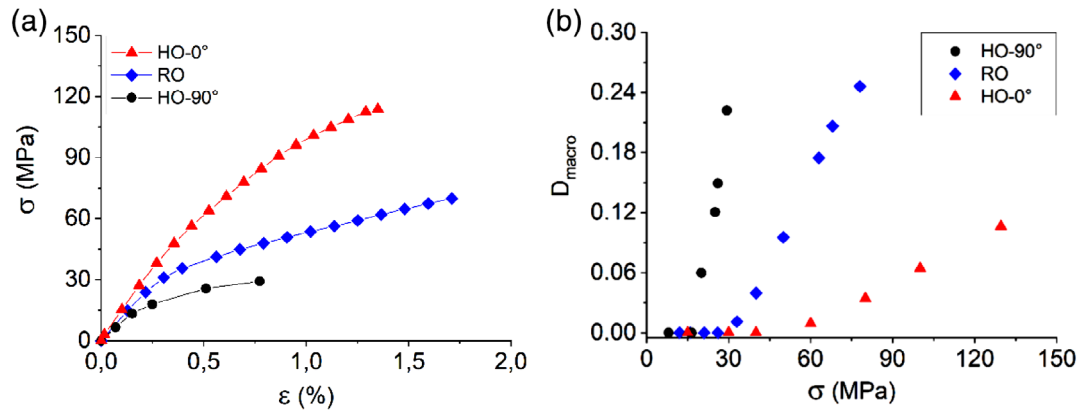


FIGURE 7 (a) Representative quasistatic stress–strain curves and (b) macroscopic damage evolution versus applied stress for HO-0°, RO, and HO-90° samples. HO, highly-oriented; RO, randomly-oriented [Color figure can be viewed at [wileyonlinelibrary.com](#)]

TABLE 3 Tensile properties of LD-SMCs

LD-SMC	<i>E</i> (GPa)	$\sigma_{\text{threshold}}$ (MPa)	$\varepsilon_{\text{threshold}}$ (%)	σ_{ultimate} (MPa)	$\varepsilon_{\text{ultimate}}$ (%)
HO-0°	12 ± 0.2	45 ± 3	0.35 ± 0.05	120 ± 5	1.35 ± 0.05
RO	10 ± 0.2	25 ± 3	0.25 ± 0.05	72 ± 5	1.70 ± 0.05
HO-90°	9 ± 0.2	20 ± 3	0.22 ± 0.05	30 ± 3	0.80 ± 0.05

Abbreviations: HO, highly-oriented; LD-SMC, low-density sheet molding compound; RO, randomly-oriented.

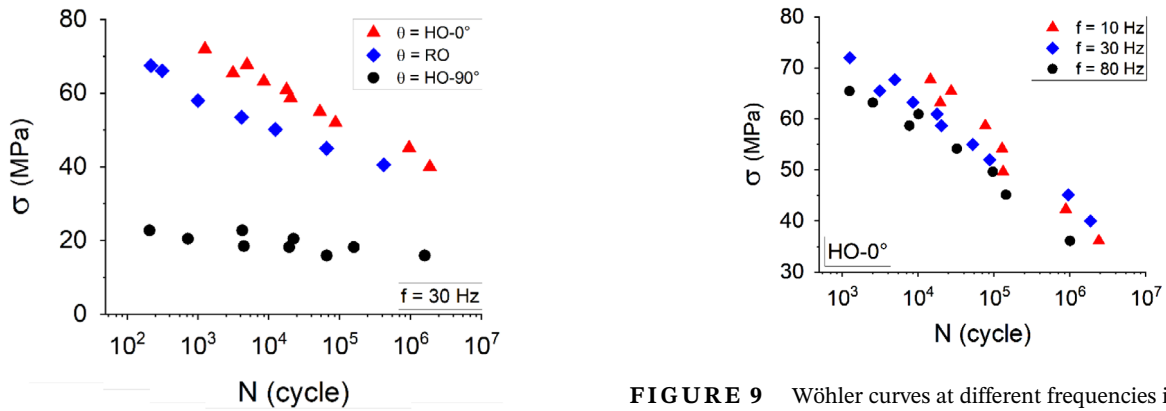


FIGURE 8 Wöhler curves for HO-0°, RO, and HO-90° samples at 30 Hz. HO, highly-oriented; RO, randomly-oriented [Color figure can be viewed at [wileyonlinelibrary.com](#)]

between the curves of 10, 30, and 80 Hz at low amplitude while at high loading amplitude, increasing frequency leads to Wöhler curves shifted to lower fatigue life. For example, for applied stress equal to 65 MPa, a variation of the frequency from 10 to 80 Hz leads to a fatigue life 30 times lower.

Independently of the loading amplitudes, frequency has a determinant influence on the fatigue life at high loading amplitudes. This phenomenon is owing to the self-heating during the fatigue test.

FIGURE 9 Wöhler curves at different frequencies in tension-tension tests for HO-0° samples. HO, highly-oriented [Color figure can be viewed at [wileyonlinelibrary.com](#)]

3.4.3 | Relative Young's modulus evolution and self-heating phenomenon

Figure 10 shows the evolution of the relative Young's modulus during tension-tension fatigue tests for HO-0°, RO, and HO-90° samples at a frequency of 30 Hz. All samples exhibit a fatigue behavior mostly governed by the MF nature due to damage phenomenon, whereas for high amplitude, the ITF is the predominant nature of the LD-SMC fatigue behavior at low cycles. The detailed analysis of MF and ITF has been presented in previous work.²

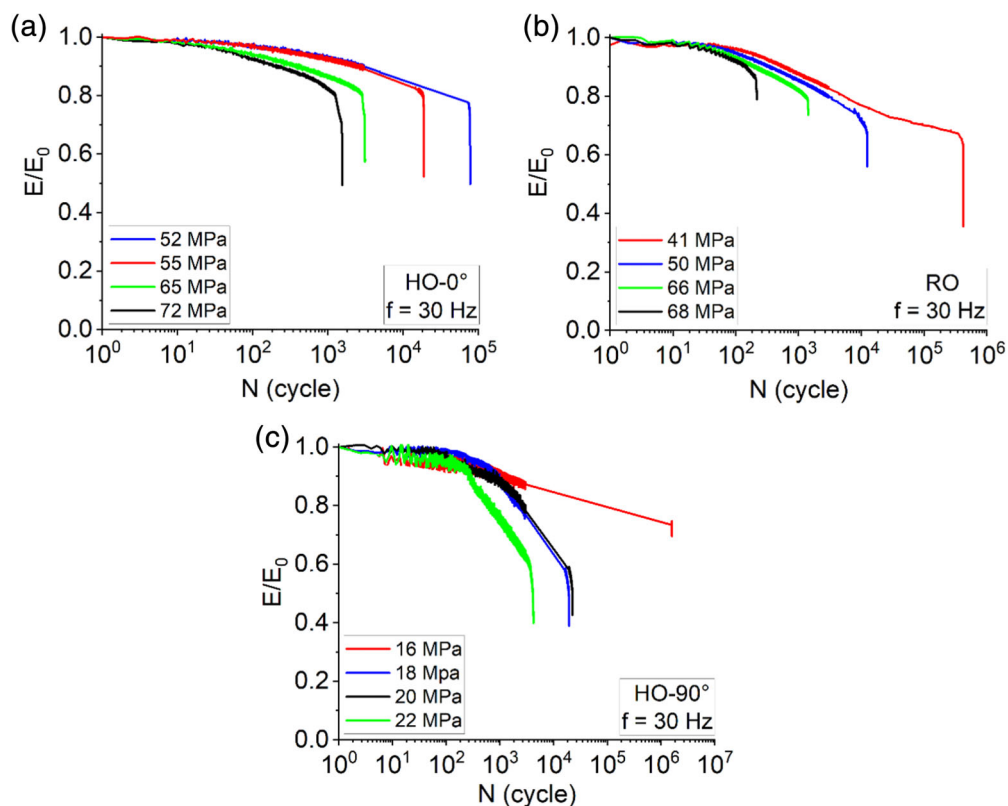


FIGURE 10 Evolutions of the relative Young's modulus (E/E_0) during fatigue tests: (a) HO-0°, (b) RO, and (c) HO-90°. HO, highly-oriented; RO, randomly-oriented [Color figure can be viewed at wileyonlinelibrary.com]

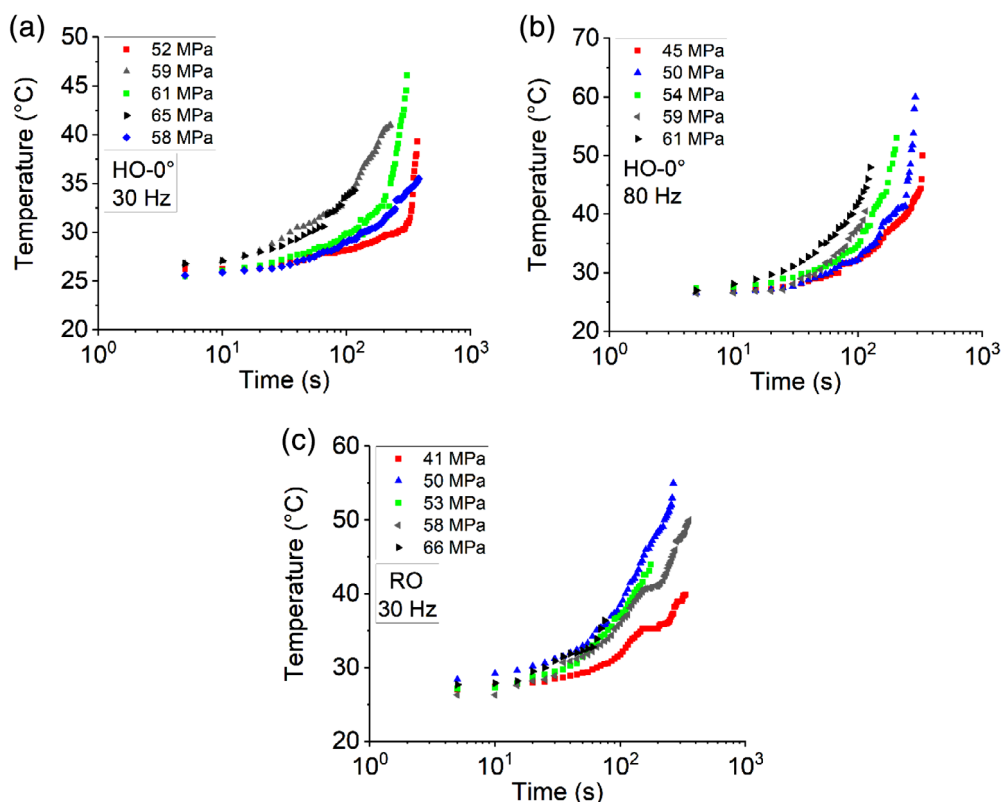


FIGURE 11 Temperature variation at different frequencies and amplitudes. HO, highly-oriented; RO, randomly-oriented [Color figure can be viewed at wileyonlinelibrary.com]

From these curves, for high loading amplitudes, the dynamic modulus decreases rapidly in a linear logarithmic regime until fracture of the specimen. For low applied amplitudes, the dynamic modulus exhibit three

decreasing regimes, a rapid one during the initial cycles, followed by a gradual one, and finally a drastic decrease just before the fracture. The significant damage kinetic is observed in the case of HO-90°.

Varying the loading conditions in terms of frequency and amplitude, the fatigue behavior of LD-SMC induces self-heating. Self-heating phenomenon influences the viscous behavior of the polyester as a function of the temperature rise level concerning material transition temperatures. The coupled effect of high loading amplitude and high frequencies generates more intensive self-heating and damage phenomena.

Figure 11(a,b) illustrate the temperature variation at different frequencies and amplitudes for HO-0° samples. The results clearly show that the temperature of LD-SMC for all fiber orientations increases when fatigue test is started while in the case of A-SMC, no significant temperature changes are noticed until 200 cycles.² This phenomenon can be related to the presence of HGSs with high surface volume proportions.

In the case of RO LD-SMC, for the test performed at 30 Hz and applied stress equal to 50 MPa, the temperature increases up to 55°C (Figure 11(c)). This temperature corresponds to the glass transition zone. At this stage, the polyester resin stiffness slightly decreases as shown in Figure 5. Therefore, the polymer matrix is subjected to extraordinary thermally activated modifications of its physical state.^{2,25}

Hence, at the microscopic scale, the fatigue behavior and failure of LD-SMC are not only due to the development of diffuse damage but also to the evolution of the viscous behavior of the polyester and the inherent brittle-ductile transition. The evolution of temperature is one of the critical parameters in fatigue.^{2,25} Maximum induced temperature can be a factor in predicting the fatigue behavior of LD-SMC and the state of polyester in terms of ductility. Figure 12 illustrates the maximum induced temperature just before failure. Figure 12(a) presents the influence of fiber orientation and Figure 12(b) shows the effect of frequency on the maximum induced temperature.

One can observe the slope of the curve at different applied amplitudes for two studied parameters: fiber orientation and frequency. As mentioned, there are two types of fatigue: MF and ITF. By considering the glass

transition temperature of about 50°C, the critical fatigue tests with ITF can be separated. For HO-90° at different loading amplitudes, the maximum temperature never reaches 50°C while. The effect of frequency shows that at 10 Hz, there is no evolution in maximum induced temperature, while for 30 and 80 Hz, the kinetic of increasing of maximum induced temperature is increased by augmentation of applied loading amplitudes.

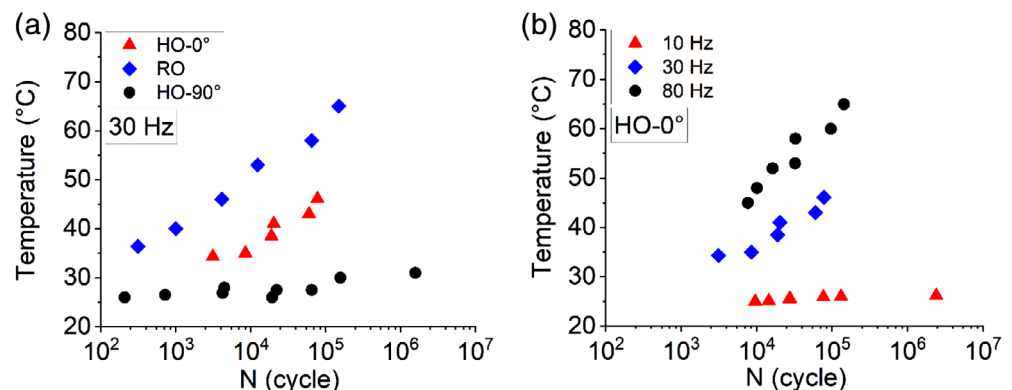
One can conclude that both fatigue behavior and fatigue life of LD-SMC composites are influenced by a coupled effect of loading amplitude and frequency, which induced thermal effect and progressive damage. In fact, the analysis of the self-heating phenomenon together with the evolution of the relative Young's modulus can be a good way to separate thermal fatigue and MF. At the same time with the temperature evolution, a stiffness loss occurs. On the other hand, the stiffness loss is affected by two factors: the self-heating (softening) of the matrix and the damage accumulation.

3.4.4 | Fatigue fracture surface

For emphasizing the coupled effect of loading amplitude and frequency at microscopic scale fracture, surface observations have been performed. Figure 13 compares the fracture surfaces of HO-0° obtained for two applied frequencies of 10 and 80 Hz. SEM analysis highlights these conclusions:

- The fracture surface observed in the case of low frequency shows that the bundles of fibers are pulled out from each other simultaneously with breakage of the more surrounding matrix (Figure 13(a,b)). Through fatigue experiments performed at 10 Hz, the self-heating remains limited leading to a more brittle fracture.
- SEM observations on the samples tested at 80 Hz, highlight smoother debonded interfaces and no

FIGURE 12 Maximum induced temperature evolution versus number of cycles: Effect of (a) fiber orientation and (b) frequency. HO, highly-oriented; RO, randomly-oriented [Color figure can be viewed at wileyonlinelibrary.com]



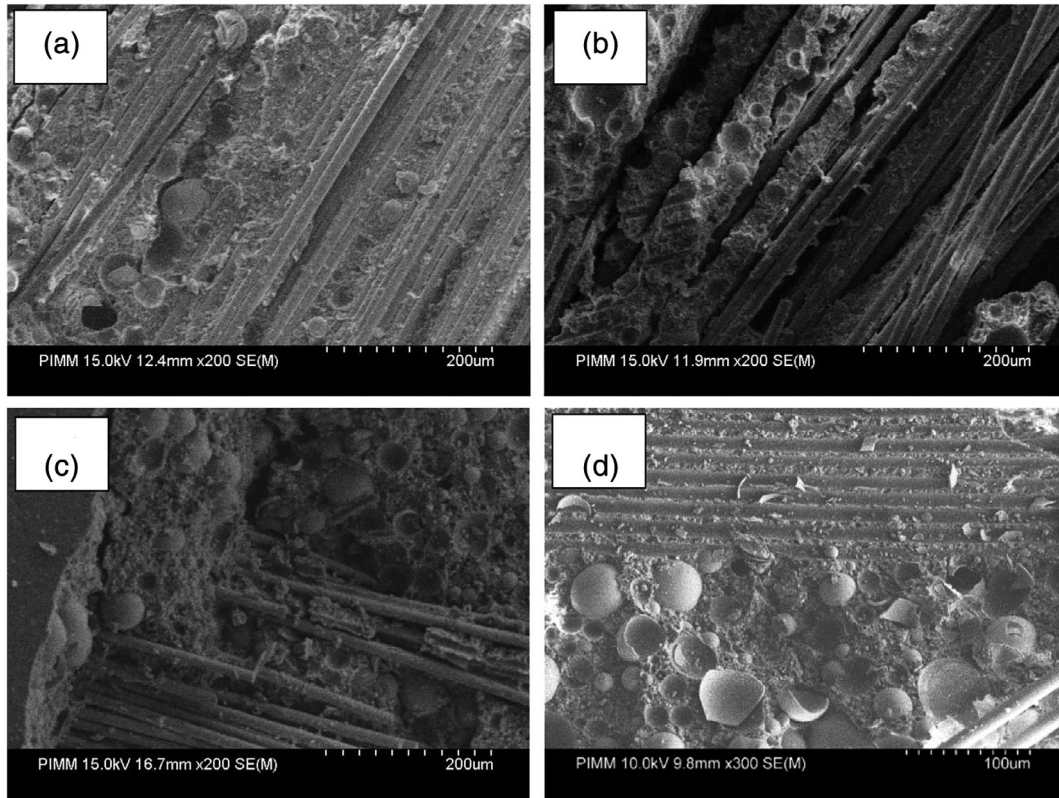


FIGURE 13 Scanning electron micrograph of fatigue fracture surface for HO-0° at $\sigma = 65$ MPa: (a,b) $f = 10$ Hz and (c,d) $f = 80$ Hz. HO, highly-oriented

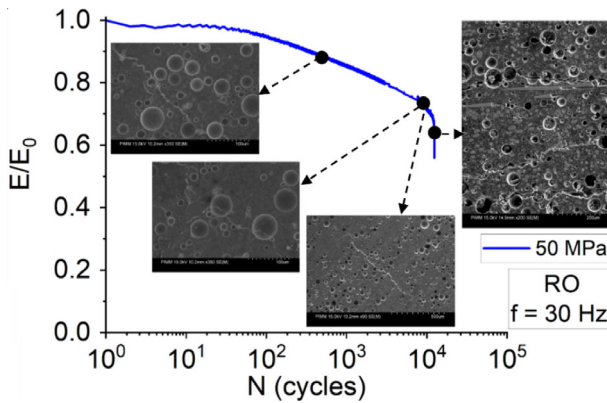


FIGURE 14 Experimental fatigue test coupled to microstructure observations for randomly-oriented sample ($\sigma = 50$ MPa/ $f = 30$ Hz) [Color figure can be viewed at wileyonlinelibrary.com]

surrounding matrix is observed on the debonded fiber/matrix interfaces (Figure 13(c,d)). Indeed, self-heating provides to the matrix softening and brings it in beyond the brittle/ductile transition.

- For all applied frequencies, HGSs participate in failure resistance. A good bond in the fiber-matrix interface exists in the LD-SMCs.

3.4.5 | Multiscale damage analysis in fatigue

In order to observe the evolution of damage development at the microstructure scale during the fatigue test of RO LD-SMC, the interrupted fatigue tests were performed coupling to microstructure observations. Figure 14 presents the results of the fatigue test for the RO sample at an applied amplitude of 50 MPa and a frequency of 30 Hz. This condition has been selected just for observing the damage phenomena, which occur during fatigue. The representative observation zone was microscopically analyzed at consecutive increasing values of the number of cycles: about 3×5 mm². The tests showed that this investigation zone is large enough to be qualitatively representative of the damage mechanisms occurring during the fatigue loading.

The first observed damage phenomenon corresponds to the debonding of the HGMs occurring in the fiber depleted zones. This leads to the propagation of matrix cracking (After about 200 cycles). For a higher value of cycles, this damage mechanism is spreading through the whole observation zone diffusely on several HGMs locations, and the early existing microcracks continue growing, and failure of HGMs was observed. Fiber-matrix

interface failure starts appearing on various bundle locations and the coalescence of the two types of microcracks can be observed. Finally, local shear deformation around the bundles leads to the pseudodelamination of the bundles near to failure.

4 | CONCLUDING REMARKS

In the present work, three microstructure configurations (RO, HO-90°, and HO-0°) of LD-SMC were prepared and submitted to tension and fatigue loadings. The main conclusion for this article is as follows: First, from the microscopic analysis that the homogeneous distribution of HGSs can be observed. HO-0° has better stiffness under tension. This means that fiber orientation distribution influences the mechanical response of LD-SMC. The later was confirmed according to the macroscopic analysis of damage indicator in terms of damage threshold and kinetic. In fatigue, the effect of fiber orientation and frequency has been analyzed. It was proved that the fatigue life is strongly influenced by the distribution of fiber orientation. The results showed that by increasing the frequency, the induced temperature is increased and as a result, the fatigue life is decreased. This phenomenon, known as self-heating, can evaluate the viscous behavior of the polyester especially in the glass transition zone. Therefore, it is necessary to investigate the viscoelastic behavior of LD-SMC. The Perez model can predict the viscoelastic behavior of polyester. Finally, to emphasize the effect of HGMs presence and fiber orientation distribution, damage mechanisms development in fatigue has been investigated at the microscopic scale. The first observed damage phenomenon corresponds to the debonding of the HGMs, which leads to the propagation of matrix cracking. For a higher value of cycles, this damage mechanism is spreading diffusely on several HGMs locations and the early existing microcracks continue growing and failure of HGMs was observed. A general conclusion to be drawn is that the presence of HGMs influences damage development and failure of LD-SMC.

ORCID

Mohammadali Shirinbayan  <https://orcid.org/0000-0002-2757-8529>

REFERENCES

- [1] A. Asadi, M. Miller, A. V. Singh, R. J. Moon, K. Kalaitzidou, *Compos. Struct.* **2017**, 160, 211.
- [2] M. Shirinbayan, J. Fitoussi, F. Meraghni, M. Laribi, B. Surowiec, A. Tcharkhtchi, *J. Reinf. Plast. Compos.* **2017**, 36, 271.
- [3] J. Njuguna, K. Pielichowski, J. R. Alcock, *Adv. Eng. Mater.* **2007**, 9(10), 835.
- [4] L. Orgéas, P. J. Dumont, Sheet molding compounds. in *Wiley Encyclopedia of Composites*, Wiley, **2011**, p. 1.
- [5] B. Huang, L. Zhao, *Compos. Part B Eng.* **2012**, 43, 3146.
- [6] A. Kraemer, S. Lin, D. Brabandt, T. Bohlke, G. Lanza, *Procedia CIRP* **2014**, 17, 772.
- [7] B. V. Gregl, L. D. Larson, M. Sommer, J. R. Lemkie, *SAE Trans.* **1999**, 797.
- [8] M. Fette, P. Sander, J. Wulfsberg, H. Zierk, A. Herrmann, N. Stoess, *Procedia CIRP* **2015**, 35, 25.
- [9] M. Oldenbo, S. Fernberg, L. A. Berglund, *Compos. A: Appl. Sci. Manuf.* **2003**, 34, 875.
- [10] M. Shirinbayan, J. Fitoussi, M. Bocquet, F. Meraghni, B. Surowiec, A. Tcharkhtchi, *Composites, Part B* **2017**, 115, 3.
- [11] M. Shirinbayan, J. Fitoussi, N. Abbasnezhad, F. Meraghni, B. Surowiec, A. Tcharkhtchi, *Composites, Part B* **2017**, 131, 8.
- [12] H. Tang, Z. Chen, G. Zhou, X. Sun, Y. Li, L. Huang, H. Guo, H. Kang, D. Zeng, C. Engler-Pinto, X. Su, *Int. J. Fatigue* **2019**, 125, 394.
- [13] C. Guster, G. Pinter, A. Mosenbacher, W. Eichlseder, *Proc. Eng.* **2011**, 10, 2104.
- [14] V. Bellenger, A. Tcharkhtchi, P. Castaing, *Int. J. Fatigue* **2006**, 28, 1348.
- [15] B. Esmaellou, P. Ferreira, V. Bellenger, A. Tcharkhtchi, *Polym. Compos.* **2012**, 33, 540.
- [16] B. Esmaellou, J. Fitoussi, A. Lucas, A. Tcharkhtchi, *Proc. Eng.* **2011**, 10, 2117.
- [17] M. Shirinbayan, J. Fitoussi, F. Meraghni, B. Surowiec, M. Bocquet, A. Tcharkhtchi, *Composites, Part B* **2015**, 82, 30.
- [18] D. Krajcinovic, S. Mastilovic, *Mech. Mater.* **1995**, 21, 217.
- [19] D. Krajcinovic, *Mech. Mater.* **1998**, 28, 165.
- [20] J. Lemaitre, J. L. Chaboche, *Mechanics of Solid Materials*, Donud, Paris **1988**.
- [21] R. Talreja, *Proc. R. Soc. London* **1981**, 378, 461.
- [22] J. Fitoussi, M. Bocquet, F. Meraghni, *Composites, Part B* **2013**, 45, 1181.
- [23] R. Renz, V. Altstadt, G. Ehrenstein, *J. Reinf. Plast. Compos.* **1988**, 7, 413.
- [24] K. Y. Hour, H. Sehitoglu, *J. Thermoplast. Compos. Mater.* **1993**, 27, 782.
- [25] Shirinbayan M., PhD thesis, Étude du comportement mécanique et de l'endommagement de divers matériaux composites smc soumis à des chargements de type dynamique, fatigue et dynamique post-fatigue. **2017**.
- [26] Laribi M., PhD thesis, Caractérisation et Modélisation du comportement micromécanique des matériaux composites SMC sous chargement thermomécanique de type quasi-statique et fatigue. **2018**.
- [27] M. F. Arif, F. Meraghni, Y. Chemisky, N. Despringre, G. Robert, *Composites, Part B* **2014**, 58, 487.
- [28] M. Schoßig, A. Zinkel, C. Bierögel, P. Pöhl, *Compos. Sci. Technol.* **2011**, 71, 257.
- [29] M. Arif, N. Saintier, F. Meraghni, J. Fitoussi, Y. Chemisky, G. Robert, *Composites, Part B* **2014**, 61, 55.
- [30] S. Tamboura, H. Sidhom, H. Baptiste, J. Fitoussi, *Matériaux & Techniques* **2001**, 89, 3.
- [31] J. Fleckenstein, K. Jaschek, A. Buter, N. Stoess, *Procedia Eng.* **2011**, 10, 390.

- [32] S. S. Wang, H. Suemasu, E. S. M. Chim, *J. Thermoplast. Compos. Mater.* **1987**, *21*, 1084.
- [33] J. Perez, *Physics and Mechanics of Amorphous Polymers*, Aa Balkema, Rotterdam **1998**.
- [34] J.-P. Pascault, H. Sautereau, J. Verdu, R. J. J. Williams, *Thermosetting Polymers*, Basel **2002**.
- [35] J. D. Ferry, *Viscoelastic Properties of Polymers*, John Wiley, New York **1970**.